Computer Physics Communications 204 (2016) 43–54

Contents lists available at ScienceDirect

Computer Physics Communications

journal homepage: www.elsevier.com/locate/cpc

Real-space finite difference scheme for the von Neumann equation with the Dirac Hamiltonian

Magdalena Schreilechner, Walter Pötz *

Institut für Physik, Karl-Franzens-Universität Graz, Universitätsplatz 5, 8010 Graz, Austria

ARTICLE INFO

Article history:
Received 3 November 2015
Received in revised form
14 March 2016
Accepted 18 March 2016
Available online 28 March 2016

Keywords:
Dirac equation
von Neumann equation
Finite-difference scheme
Staggered grid
Fermion doubling
Topological insulator

ABSTRACT

A finite difference scheme for the numerical treatment of the von Neumann equation for the (2 + 1)D Dirac Hamiltonian is presented. It is based on a sequential left–right (ket–bra) application of a staggered space–time scheme for the pure-state Dirac equation and offers a numerical treatment of the general mixed-state dynamics of an isolated quantum system within the von Neumann equation. Thereby this direct scheme inherits all the favorable features of the finite-difference scheme for the pure-state Dirac equation, such as the single-cone energy–momentum dispersion, convergence conditions, and scaling behavior. A conserved functional is identified. Moreover this scheme is shown to conserve both Hermiticity and positivity. Numerical tests comprise a numerical analysis of stability, as well as the simulation of a mixed-state time-evolution of Gaussian wave functions, illustrating Zitterbewegung and transverse current oscillations. Imaginary-potential absorbing boundary conditions and parameters which pertain to topological insulator surface states were used in the numerical simulations.

1. Introduction

1.1. The Dirac equation and single-cone numerical schemes

The Dirac equation is the fundamental wave equation for relativistic fermions and has been employed in practical all fields of theoretical physics, from the standard model of elementary particle physics, atomic, molecular, and condensed-matter physics to astrophysics and cosmology [1–5]. Recent developments in condensed matter physics, in particular, have renewed the interest in (2 + 1)D versions (2 space- and one time-coordinates) of the Dirac equation to describe the low-energy spectrum of graphene and surface-states of topological insulators (TIs) [6–11].

In the numerical modeling of Dirac fermions on a lattice, for example in lattice quantum-chromodynamics (QCD), the effect of fermion doubling has caused considerable difficulties [12,13]. It arises from the implementation of first-order derivatives by finite-difference approximations using twice the lattice constant. Recently we have identified a class of staggered grids on which fermion doubling can be avoided in arbitrary space dimensions, with explicit schemes given for the (1 + 1)D, (2 + 1)D, and (3 + 1)D case [14,15]. To our knowledge this is the first class of finite-difference schemes for the Dirac operator which displays a single energy–momentum cone only and is explicit (local), i.e. can be executed locally mesh-point by mesh-point. The scheme scales linearly with the number of grid points and allows a gauge-invariant formulation of electromagnetic fields on the lattice. Moreover, the underlying grid can be used in any space–time formulation involving the Dirac operator, such as density matrix and Green's function approaches, while yielding a single Dirac cone.

In this work we extend the single-cone scheme for the (2 + 1)D time-dependent Dirac equation for pure states to a numerical scheme for the mixed-state time-evolution under the Dirac Hamiltonian H in (2 + 1)D which is described by the von-Neumann equation

$$i\hbar\dot{\rho} = H\rho - \rho H = [H, \rho]\,. \tag{1}$$

It lends itself to extensions which describe open and dissipative quantum systems, such as the simulation of quantum transport on TI surfaces at energies near the Dirac point [16,17]. The scheme to be presented below utilizes the staggered grid of Ref. [15] to define centered differences over a single lattice spacing, thereby eliminating the very source for fermion doubling from the start. It is the adoption of R. Hammer's staggered grid and the representation of partial derivatives using single lattice spacings which ensures a single-cone dispersion on the grid and links this work to Ref. [15]. In Sections 1.2 and 1.3, respectively, we review the continuum space–time representation of the Dirac von Neumann equation and select the placement of the density matrix components on a

* Corresponding author.
E-mail address: walter.poetz@uni-graz.at (W. Pötz).

http://dx.doi.org/10.1016/j.cpc.2016.03.005
0010-4655/

staggered grid which is the key for eliminating fermion doubling. In Section 2 we formulate the ket–bra numerical scheme and prove its main properties. It treats the time derivative of the density operator ρ within the product rule as indicated by the commutator on the r.h.s. of Eq. (1): apply H from the left and therewith propagate the ket in time, apply H from the right and therewith propagate the bra in time, and form the difference. In Section 3 we explore the trace conservation properties numerically and provide elementary examples for mixed-state dynamics of Dirac fermions for an illustration of the scheme.

1.2. The continuum formulation of the von Neumann equation for the $(2+1)$D Dirac Hamiltonian

We consider the effective model Hamiltonian which accounts for the energy spectrum of TI surface states near the Dirac point [7][1]

$$H = v\,(\boldsymbol{\sigma}\times\mathbf{P})\,|_z + m(X,Y,t)\sigma_z + V(X,Y,t)\mathbb{1}_2. \tag{2}$$

Here, $v, \sigma_i, i = x, y, z$, and $\mathbf{P}$, respectively, denote the Fermi velocity, the Pauli matrices [2], and the momentum operator. $\mathbb{1}_2$ is the 2×2 unit matrix. $m(X,Y,t)$ and $V(X,Y,t)$, respectively, denote the position- (X,Y) and time- (t) dependent "mass" and scalar potential term. Using the abbreviation[2]

$$\partial_\pm = v\left(P_y \pm iP_x\right)$$

and (omitting space–time arguments)

$$m_\pm = V \pm m$$

this Hamilton operator takes the form of a 2×2 matrix

$$H = \begin{pmatrix} m_+ & \partial_+ \\ \partial_- & m_- \end{pmatrix}.$$

Inserted into the von Neumann equation (1) one obtains a set of first-order partial differential equations in space and time for the density operator elements ρ_{ij}, conveniently written as the 2×2 matrix identity (see Box I).

Note that, as in the original von Neumann equation, Hamilton matrix operator elements to the right of the density operator matrix elements act to the left (and vice versa). The two-component nature of the spin-1/2 Dirac fermion suggests this 2×2 form. Choosing a continuous space representation for the orbital degrees of freedom one arrives at the equation given in Box II.

Here we omit the time variable t, common to all terms, for brevity, and use the real-space versions of the abbreviations defined above, *i.e.*,

$$\partial_\pm = \frac{\hbar v}{i}\left(\partial_y \pm i\partial_x\right), \qquad \partial'_\pm = \frac{\hbar v}{i}\left(\partial_{y'} \pm i\partial_{x'}\right)$$

and (including arguments)

$$m_\pm(x,y,t) = V(x,y,t) \pm m(x,y,t).$$

Note that in the real-space representation we have

$$\begin{aligned}\langle\Psi_j|\left(P_y \pm iP_x\right)\,|\,x,y\rangle &= \langle\left(P_y \mp iP_x\right)\Psi_j\,|\,x,y\rangle \\ &= \langle x,y\,|\,\left(P_y \mp iP_x\right)\Psi_j\rangle^* = -\partial_\pm\Psi_j(x,y)^*.\end{aligned}$$

1.3. Placement onto the space–time grid

The task at hand now is to develop a space–time finite-difference approximation to Eq. (4) which avoids fermion doubling.

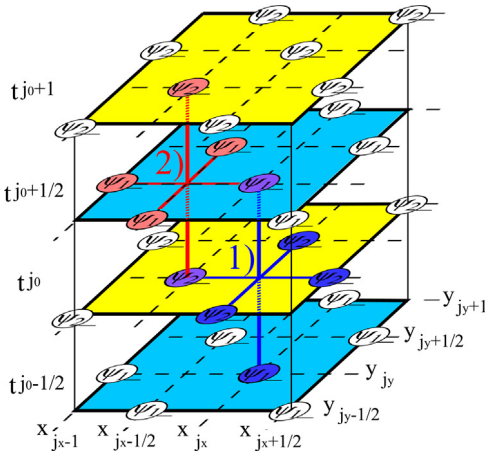

Fig. 1. (Color online) Sketch of the staggered grid needed to propagate a two-component spinor Ψ by one time step Δ_t. Placing upper and lower components onto the adjacent time sheets, respectively, $t^{j_o-\frac{1}{2}}$ and t^{j_o} allows the propagation to the next pair of time sheets via spatial derivatives, represented by single lattice spacings (Δ_x and Δ_y), in two steps: first the upper spinor component from subgrid $\mathcal{G}_1^{j_o-\frac{1}{2}}$ to $\mathcal{G}_1^{j_o+\frac{1}{2}}$, then the lower spinor component from subgrid $\mathcal{G}_2^{j_o}$ to $\mathcal{G}_2^{j_o+1}$.

This is achieved by using the staggered grid introduced in an earlier paper to accommodate the real-space density matrix in which upper and lower spinor component(s) are placed on two adjacent time-sheets [15]. Fig. 1 gives a sketch of the grid and the propagation by one time step.

The proper implementation is found by inspection of the density operator for a pure state spinor. In $(2+1)$D one has a pure-state ket $|\Psi\rangle = \binom{\psi_1}{\psi_2}$ and the corresponding ket–bra projector for the representation as a density operator

$$\rho = |\Psi\rangle\langle\Psi| = \begin{pmatrix}\psi_1 \\ \psi_2\end{pmatrix}\begin{pmatrix}\psi_1^* & \psi_2^*\end{pmatrix} = \begin{pmatrix}\psi_1\psi_1^* & \psi_1\psi_2^* \\ \psi_2\psi_1^* & \psi_2\psi_2^*\end{pmatrix}. \tag{5}$$

In general, the density operator being Hermitian, trace-one, and positive may be cast into the form [16]

$$\rho = \sum_k \gamma_k |\Psi_k\rangle\langle\Psi_k|, \tag{6}$$

where $|\Psi_k\rangle$ are wave functions normalized to one, and $0 \le \gamma_k \le 1$, $\gamma_k \in \mathbb{R}$ with $\sum_k \gamma_k = 1$.

This shows that the Pauli indices of ρ, 1 and 2 respectively, take the face-centered rectangular ψ_1-grid ($\mathcal{G}_1$) and ψ_2-grid ($\mathcal{G}_2$) position. For a single-cone representation the latter are [15]

$$\begin{aligned}\psi_1(j) \quad \text{with } j \in \mathcal{G}_1 = \big\{&(j_x, j_y, j_o - 1/2),\ (j_x + 1/2, j_y \\ &+ 1/2, j_o - 1/2)\,|\,j_\nu \in \mathbb{Z},\ \nu = x, y, o\big\}, \\ \psi_2(j) \quad \text{with } j \in \mathcal{G}_2 = \big\{&(j_x + 1/2, j_y, j_o),\ (j_x, j_y + 1/2, j_o)\,| \\ &j_\nu \in \mathbb{Z},\ \nu = x, y, o\big\}.\end{aligned}$$

Here the time index is labeled o. Note that, for given time, ψ_1 and ψ_2 are placed onto adjacent time sheets, respectively, $j_0 - 1/2$ and j_0. Each time sheet contains a rectangular face-centered spatial grid, symmetrically staggered relative to the ones on the two adjacent time sheets, such that symmetric difference quotients replace the respective partial derivatives on the grid, as sketched in Fig. 1. The grid spacings are denoted by Δ_x, Δ_y, and $\Delta_o = v\Delta_t$. We also introduce the associated grids

$$\begin{aligned}\bar{\mathcal{G}}_1 &= \big\{(j_x, j_y, j_o),\ (j_x + 1/2, j_y + 1/2, j_o)\,|\,j_\nu \in \mathbb{Z},\ \nu = x, y, o\big\}, \\ \bar{\mathcal{G}}_2 &= \big\{(j_x + 1/2, j_y, j_o + 1/2),\ (j_x, j_y + 1/2, j_o + 1/2)\,| \\ &\qquad j_\nu \in \mathbb{Z},\ \nu = x, y, o\big\}.\end{aligned}$$

[1] Note that the TI representation differs from the standard representation used in Ref. [15], however, simply shifting $P_x \to P_y$ and $P_y \to -P_x$ converts the latter to the former.

[2] For now, the electromagnetic vector potential is set equal to zero.